

Contents lists available at ScienceDirect

Petroleum Science

journal homepage: www.keaipublishing.com/en/journals/petroleum-science



Original Paper

Hydrophobic epoxy resin coated proppants with ultra-high selfsuspension ability and enhanced liquid conductivity



Fan Fan, Feng-Xia Li, Shou-Ceng Tian, Mao Sheng, Waleed Khan, Ai-Ping Shi, Yang Zhou*, Ouan Xu**

State Key Laboratory of Shale Oil and Gas Enrichment Mechanisms and Effective Development, National Energy Shale Oil Research and Development Center, Harvard SEAS-CUPB Joint Laboratory on Petroleum Science, China University of Petroleum (Beijing), Beijing, 102249, China

ARTICLE INFO

Article history: Received 7 February 2021 Accepted 15 July 2021 Available online 3 September 2021

Edited by Yan-Hua Sun

Keywords:
Coated proppant
Hydrophobic property
Self-suspension
Conductivity

ABSTRACT

Proppant is a key material for enhancing unconventional oil and gas production which requires a long distance of migration and efficient liquid conductivity paths within the hydraulic fracture. However, it is difficult to find a proppant with both high self-suspension ability and liquid conductivity. Here, a simple method is developed to coat epoxy resin onto the ceramic proppant and fabricate a novel coated proppant with high hydrophobicity, self-suspension, and liquid conductivity performance. Compared with uncoated ceramic proppants, the epoxy resin coated (ERC) proppant has a high self-suspension ability nearly 16 times that of the uncoated proppants. Besides, the hydrophobic property and the liquid conductivity of the ERC proppant increased by 83.8% and 16.71%, respectively, compared with the uncoated proppants. In summary, this novel ERC proppant provides new insights into the design of functional proppants, which are expected to be applied to oil and gas production.

© 2021 The Authors. Publishing services by Elsevier B.V. on behalf of KeAi Communications Co. Ltd. This is an open access article under the CC BY-NC-ND license (http://creativecommons.org/licenses/by-nc-nd/4.0/).

1. Introduction

To efficiently increase hydrocarbon recovery from unconventional reservoirs, hydraulic fracturing (HF) is known as an effective method to increase the output of a single well (Cao et al., 2019; Chen et al., 2015; Jia et al., 2012; Witte et al., 2010). Proppant is an essential material in fracturing construction, which is used to provide structural support for the fractures to remain conductive (Al-Muntasheri et al., 2017; Dong et al., 2020; Shiozawa and McClure, 2016; Wen et al., 2007). Once a fracture is created, the slurry composed of the fracturing fluid and proppants is injected to provide efficient flow of hydrocarbons from fractures to the wellbore (Kulkarni and Ochoa, 2012; Tomac and Gutierrez, 2015; Hu et al., 2013). Currently, the commercial fracturing proppants in the market mainly include quartz sand proppants, ceramic, and coated proppants (Gomez et al., 2017; Liang et al., 2016; Zoveidavianpoor and Gharibi, 2015). The price of guartz sand proppants is relatively low; however, the high crushing rate, low

compressive strength, and sphericity of these proppants make them unsuitable for certain operations (Gu et al., 2015; Kondash and Vengosh, 2015; Ma et al., 2016). The strength of ceramic proppants is higher than quartz sand proppants, while the disadvantages of ceramic proppants included high density, cost, and construction risk (Moghadasi et al., 2019; Palisch et al., 2015). The coated proppant uses the principle of surface modification to improve the performance of the proppant by simply coating conventional sand. The hydrophobic proppants (Liu et al., 2015), selfpolymerizing proppants (Fu et al., 2016b; Zhang et al., 2017), selfsuspending proppants (Cao et al., 2020), magnetic proppants (Bogacki and Zawadzki, 2019; Liu et al., 2019; Pangilinan et al., 2016), carrier proppants (Liang et al., 2016) that have been developed now, utilize the principle of surface modification. The coating materials and modification technologies are optimized, allowing the proppants to have enhanced efficiencies (Chen et al., 2012; Fan et al., 2018).

Among the different types of proppants, the research on hydrophobic proppants has gradually deepened. Since the hydrophobicity of the proppant has a significant impact on the recovery efficiency of hydraulic fracturing, it is necessary to improve the hydrophobicity of the proppant. According to wettability, proppants can be divided into hydrophilic, neutral, and hydrophobic

E-mail addresses: zhouyang@cup.edu.cn (Y. Zhou), xuquan@cup.edu.cn (Q. Xu).

^{*} Corresponding author.

^{**} Corresponding author.

proppants (Liu, 2011). The surface of conventional quartz sand and ceramic is hydrophilic, while fracturing fluids used in oilfields are usually water-based fracturing fluids, leading to premature flooding of oil wells (Liang et al., 2016; Yang et al., 2019). Currently, the preparation methods of hydrophobic proppants mainly include surfactant modification (Yan and Wang, 1993), silane coupling agent modification (Fu et al., 2016a: Jung and Choi, 2009: Liu et al., 2015), and resin coating modification (Yang et al., 2019), Surfactants and silane coupling agents can self-assemble on the surface of the proppant to form a monomolecular hydrophobic layer, which can effectively alter the hydrophilic/hydrophobic properties of the proppant. Compared with the original proppant, its crush resistance has not been effectively improved (Liu et al., 2015). Resincoated proppant increases the hydrophilic/hydrophobic properties by coating a layer of resin on the surface of the proppant (Chen et al., 2015).

In this work, we have successfully designed and fabricated an epoxy resin-coated proppant with a simple method. The epoxy resin coats the surface of the proppant to form a core-shell structure (Fig. 1a). The surface of the epoxy resin coated (ERC) proppant is smooth, at the same time, the sphericity of the ERC proppant is close to 1. Fig. 1b shows the schematic diagram of the migration and distribution of proppant in the hydraulic fracture, uncoated normal ceramic proppants more likely to sediment at the entrances of shale fractures. Compared with uncoated proppants, ERC proppants have improved a variety of properties, including hydrophobic properties, liquid conductivity and self-suspension ability, etc. This new type of proppant helps to promote the migration of proppant in fractures and improve the support effect on fractures.

2. Materials and methods

2.1. Experimental materials

The experimental materials mainly include ceramic proppant (40/80 mesh), epoxy resin E51 and supporting curing agent, guar gum (West Asia reagent), ethanol absolute (≥99.7%, Tianjin Zhiyuan).

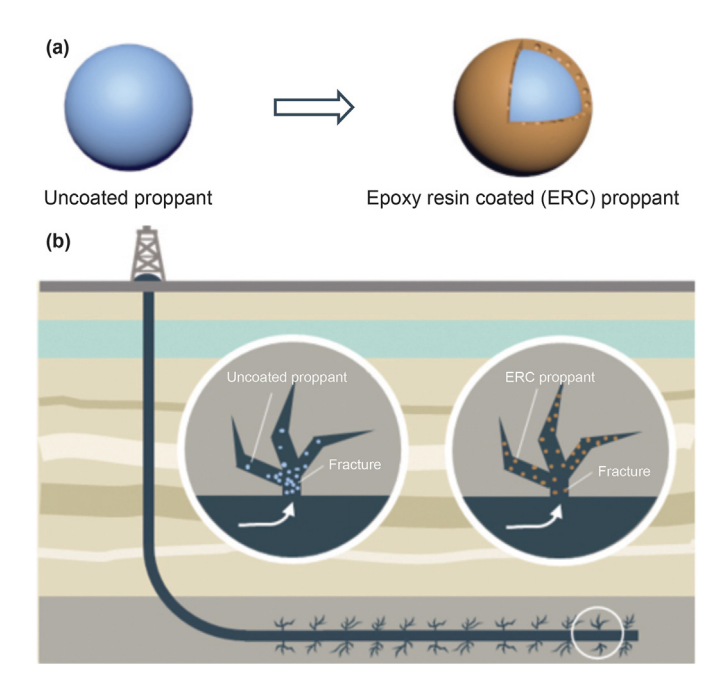


Fig. 1. (a) Core-shell structure of proppant. (b) The migration of proppant in fracturing fractures.

2.2. Preparation of resin-coated proppant

Epoxy resin E51 and supporting curing agent were mixed in a mass ratio of 2:1 under stirring at room temperature. After stirring for 5 min, the ceramic proppant was poured into the solution of epoxy resin E51 and curing agent and the mixture was stirred thoroughly. After that, the proppant in the resin was taken out and tiled in an oven, and then dried at 70 $^{\circ}$ C for 6 h. Finally, the cooled block-shaped coated proppant was ground at 2000 rpm for 1 min in a grinder.

2.3. Sedimentation experiment

A guar gum solution with a mass fraction of 0.2 wt% was prepared. One gram of ERC proppants was slowly poured into a beaker containing 500 mL of guar gum solution (0.2 wt%). The solution was kept stirring at different rates for 5 min. Subsequently, 1 g of uncoated proppants was poured into the solution under the same conditions. After stirring for 5 min the proppants suspended on the solution surface were collected and dried. And the self-suspension ability can be calculated as follows:where S is the self-suspension ability, $m_{\rm ps}$ is the mass of proppants on the surface of the solution, $m_{\rm pt}$ is the total mass of proppants in the solution.

2.4. Characterization

A scanning electron microscope (SEM, Zeiss Sigma500) and an energy-dispersive X-ray spectrometer (EDS, Bruker XFlash 6/30) were used to capture SEM and EDX images of the sample. Atomic force microscopy (AFM) imaging was performed on a Bruker Dimension Icon with Scan Asyst. The contact angles between the proppant and water, guar gum solution (0.2 wt%), and Daqing crude oil were measured with an optical contact angle measuring instrument (SDC-200). Liquid conductivity tester FCS-842 was used to measure liquid conductivity of the proppant.

3. Results and discussion

The surface roughness of the proppant has a serious impact on fouling for crystals would adsorb and gather on the surface of the proppant with higher roughness to block the fracture. SEM images of the surface morphology of the uncoated ceramic proppant (uncoated proppant) and the ERC proppant are shown in Fig. 2. It can be seen from Fig. 2, the surface of the uncoated ceramic proppant is rough and has many holes. The sphericity of the ERC proppant is improved and the surface is significantly smoother than the ceramic proppant. As shown in the EDX results of uncoated ceramic proppant (Fig. 3a), aluminum (Fig. 3c) and silicon (Fig. 3d) elements can be found on the surface, while almost no carbon element (Fig. 3b). For the ERC proppant, aluminum (Fig. 3f) and silicon (Fig. 3g) contents are reduced, and carbon (Fig. 3h) element can be observed on the surface. The change in the element content of the proppant surface tested by the EDX mapping proves that resin has been coated on the surface of the proppant.

3.1. Hydrophobic properties

The hydrophobic performance of the proppant was determined through measuring the contact angle between proppant and water, and the dropped droplet was 1 μ L. As shown in Fig. 4a and Fig. S1 (see electronic supplementary material), compared with the uncoated ceramic proppant, the hydrophobic performance of the ERC proppant is improved. The contact angle between water and the ERC proppant is 91.7°, while the contact angle between water and the uncoated ceramic proppant is only 49.9°. The contact angles

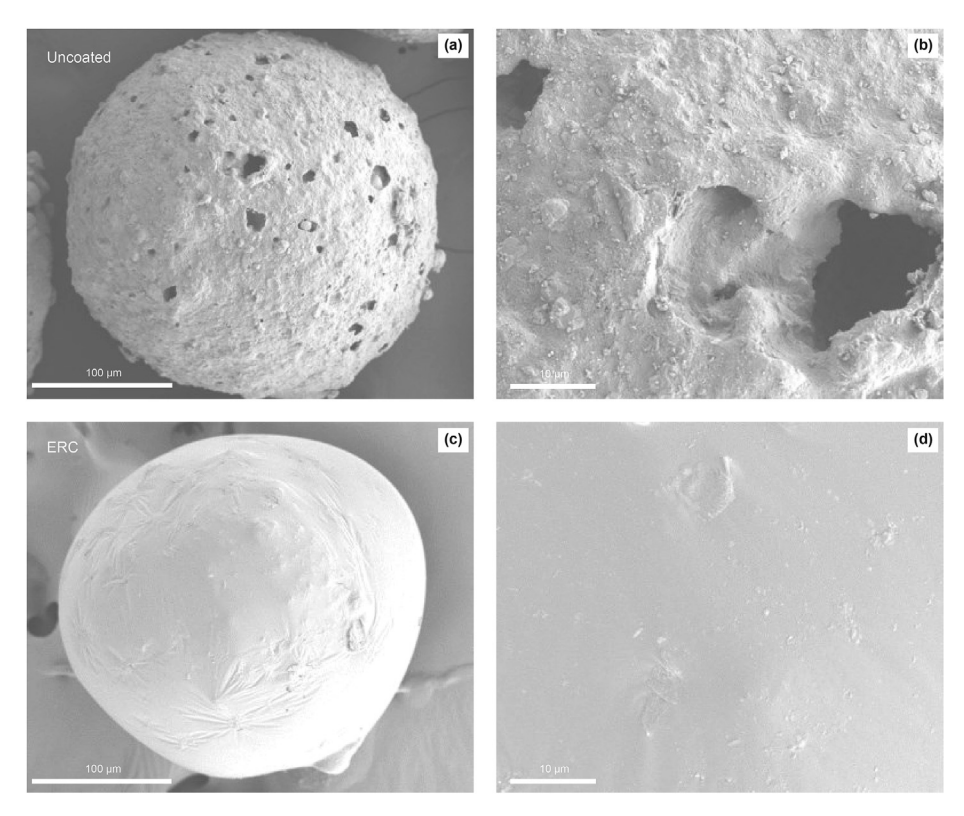


Fig. 2. SEM images of uncoated and ERC proppants. (a) (b) SEM images of the uncoated proppant. (c) (d) SEM images of the ERC proppant.

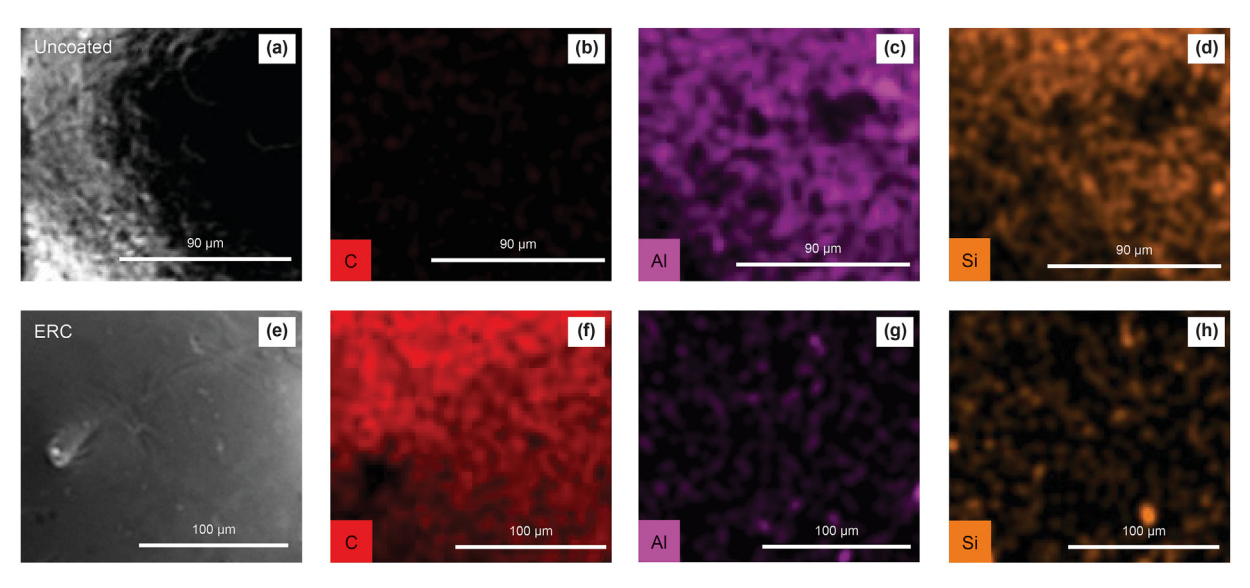


Fig. 3. EDX mapping of the uncoated and ERC proppants. (a, e) SEM images of the uncoated and ERC proppants. (b, f) Carbon on the surface of the uncoated and ERC proppants. (c, g) Aluminum on the surface of the uncoated and ERC proppants. (d, h) Silicon on the surface of the uncoated and ERC proppants.

between the guar gum solution (0.2 wt%) and proppants were also measured (Fig. 4b). The contact angle is 83.5° for the uncoated proppant and for the ERC proppant its value reaches approximately 106.5°. To test the lipophilicity of the proppants, the contact angle between the Daqing crude oil and proppants were measured. As shown in Fig. 4c, the contact angles of oil on the surface of the uncoated and ERC proppants are 19.0° and 15.9°, respectively. In conclusion, the contact angles of water and the guar gum solution on the ERC proppant surface increase by 83.8% and 27.46%, respectively, compared with the uncoated proppant; while the

lipophilic contact angle increases by 16.22%. It is can be seen that the ERC proppant improves the hydrophobicity of the proppant while maintaining high lipophilicity. The epoxy group of epoxy resin is a hydrophobic group, which enhances the hydrophobicity of the ERC proppant (Syakur et al., 2017). When the oil-water two-phase mixture passes, the proppant can restrain the flow of the water phase to the greatest extent without affecting the flow of the oil and gas phases, thereby reducing the water content of the fluids produced from the oil well (Fu et al., 2016a; Liu et al., 2015). At the same time, hydrophilic proppants are easier to scale than

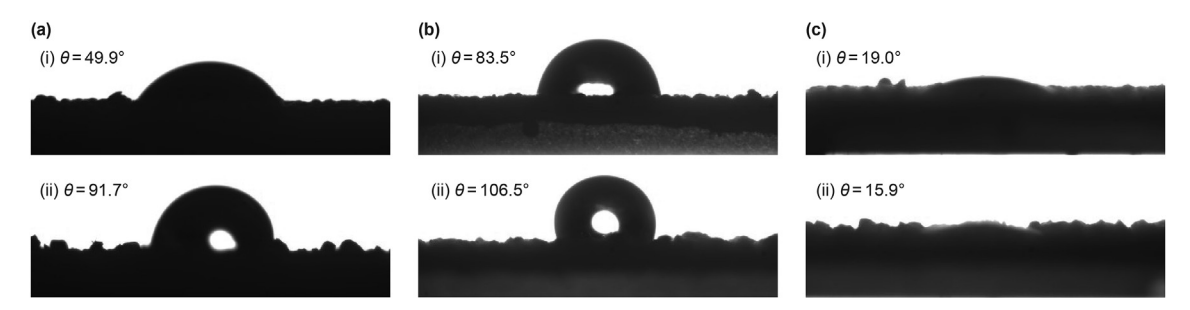


Fig. 4. (a) Contact angle between water and uncoated proppant (i) and ERC proppant (ii). (b) Contact angle between 0.2 wt% guar gum solution and uncoated proppant (i) and ERC proppant (ii). (c) Contact angle between Daqing crude oil and uncoated proppant (i) and ERC proppant (ii).

hydrophobic proppants, and the smaller the wetting angle, the greater the tendency of proppants for scaling (Samaha et al., 2012; Dong et al., 2019). The hydrophobic coating of the ERC proppant can provide excellent shear strength and make the fracturing fluid flow better, thereby improving the overall liquid conductivity.

3.2. Adhesion ability

The adhesion ability of ERC proppants and uncoated ceramic proppants were determined with an atomic force microscope (AFM). Fig. 5a gives the variations of adhesion forces under different preload conditions when the contact time was fixed at 0.5 s. The adhesion force of the ERC and uncoated proppants both increase as the load force grows from 0.5 μN to 3.0 μN (interval is $0.5~\mu N$), but the growth rate of the ERC proppants is greater. Moreover, as the load force increases, the adhesion force of ERC proppants is much higher than the uncoated proppants in different load force conditions, which is 238.34%, 411.86%, 593.60%, 479.42%, 505.67%, 587.11%, respectively. The adhesion force versus contact time is shown in Fig. 5b, where the contact time increases from 0.5 s to 3 s, while the load force was kept at 1.5 μ N. The adhesion forces of the ERC and uncoated proppants are almost constant when the contact time increases. Under different contact time conditions, the adhesion forces of ERC proppants change by 498.50%, 502.62%, 635.23%, 621.86%, 664.24%, 638.35%, respectively, compared with the uncoated proppant. The typical AFM force (known as force curve) is illustrated in Fig. 6, the adhesion force is determined by the difference of extended and retracted force curves. ERC proppants have a higher adhesion force than

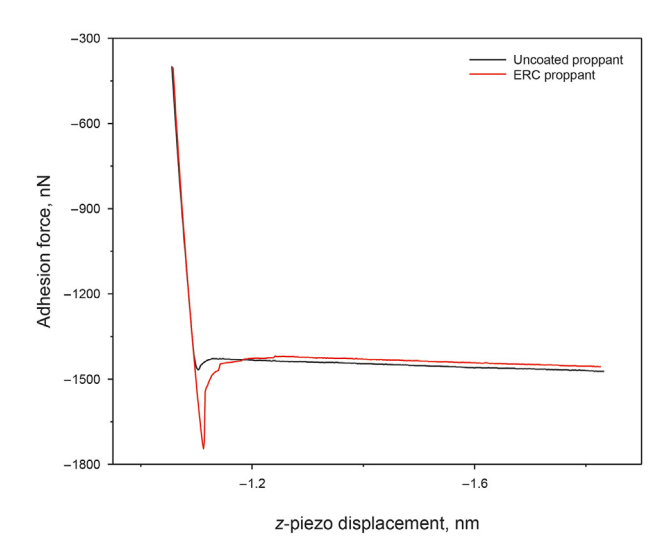


Fig. 6. Typical AFM force curve in adhesion measurement for a load force of 2 μN and a contact time of 0.5 s.

uncoated proppants, so they adhere to the fracture surface more easily, and they will be more densely distributed in the fracture. As the width of the proppant agglomerates increases, the porosity and permeability of the proppant also increase, this may be beneficial to improve the liquid conductivity of the proppant.

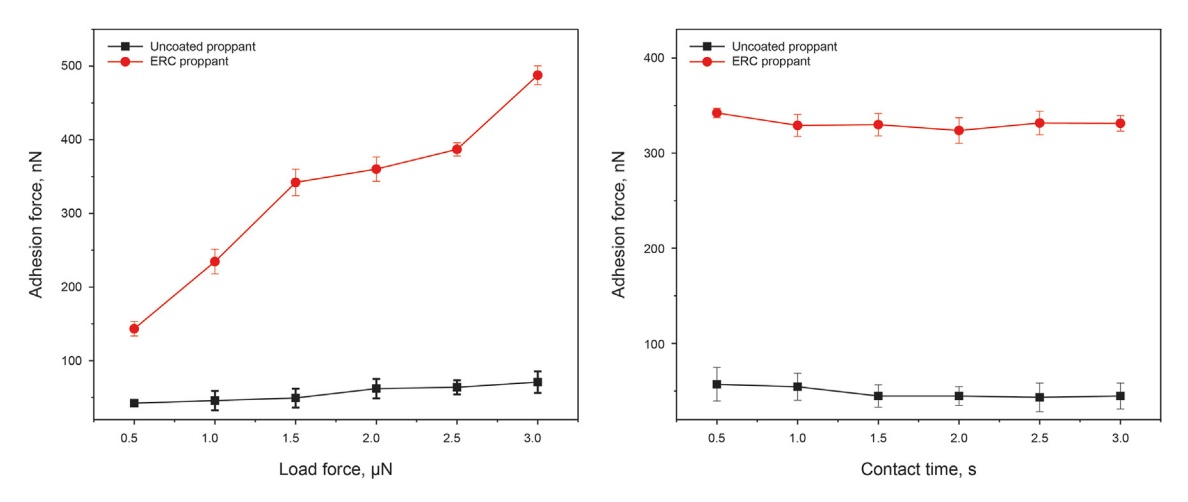


Fig. 5. (a) Adhesion performance of the uncoated and ERC proppants at different load forces. (b) Adhesion performance of the uncoated and ERC proppants of different contact times.

3.3. Liquid conductivity

Fig. 7 reveals the liquid conductivity of the proppants under different closure pressures from 5 MPa to 50 MPa when the proppant concentration and flowrate were fixed at 6 kg/m² and 3 mL/min, respectively. The liquid conductivity of both the ERC proppant and the uncoated proppant decreases as the closure stress increases. At the closure stress of 5, 10, 20, 30, 40, and 50 MPa, the liquid conductivity of the ERC proppant is 6.29%, 5.02%, 15.84%, 7.93%, 16.71%, and 15.64% higher than the uncoated proppant,

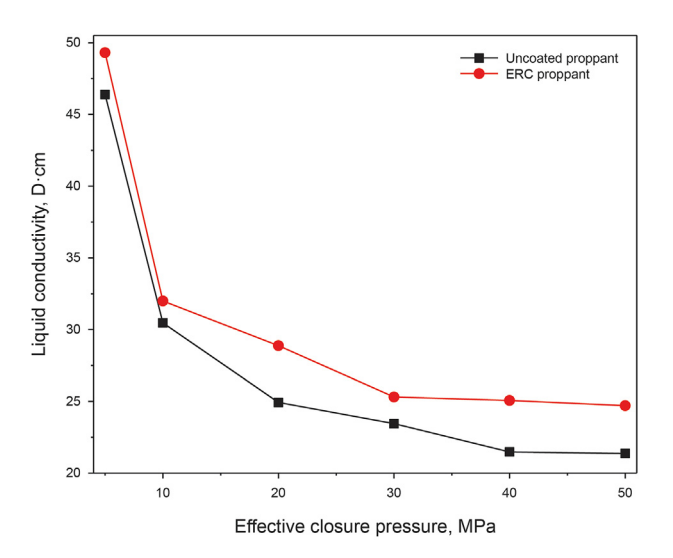


Fig. 7. Liquid conductivity of the uncoated and ERC proppants under different closure pressures.

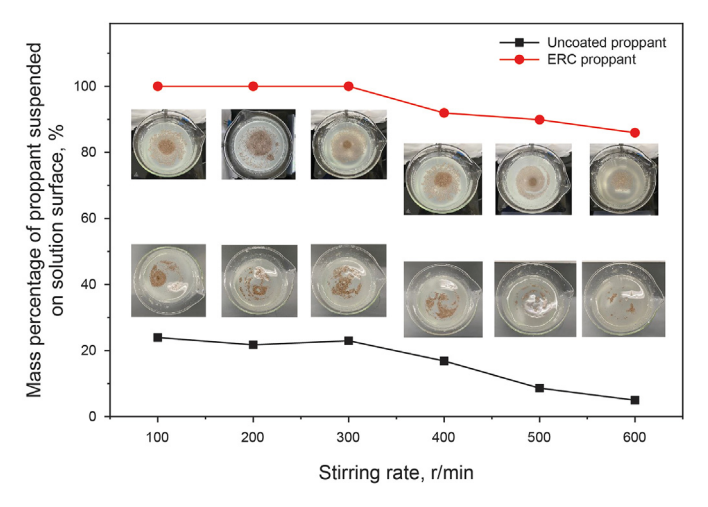


Fig. 8. Self-suspension ability of the ERC and uncoated proppants.

respectively. It can be seen that the liquid conductivity increases more proportionally under high closure stresses. Due to the epoxy resin coating on the ERC proppant surface, the coating effect of the external resin film reduces the blockage caused by particle migration, and the ERC proppants can be applied to deep wells even if the internal aggregate is broken at high closure pressures. The improvement of the liquid conductivity of the ERC proppant can be attributed to the reduction of surface roughness, the improvement of hydrophobic performance, and enhancement of adhesion force.

3.4. Sedimentation behavior

To test the self-suspension ability of the ERC proppant, sedimentation experiments were conducted. Guar gum was used to simulate underground fracturing fluid (Barati and Liang, 2014). In sedimentation experiments, the results of the mass fractions of the ERC proppant and uncoated proppant suspended on the surface of the solution are shown in Fig. 8. When the stirring rate is in the range of 100–300 r/min (interval 100 r/min), the ERC proppant almost all suspends on the surface of the guar gum solution. When the stirring rate is 400-600 r/min, the mass percentage of the ERC proppant suspended on the surface of the solution falls within the range of 91.92%-85.92%. Under the same operating conditions, as the stirring rate increases from 100 to 600 r/min, the mass percentage of the uncoated ceramic proppant suspended on the solution surface decreases from 23.94% to 4.97%. The self-suspension ability of the ERC proppant improves significantly compared to the uncoated proppant. When the stirring rate is maintained at 600 r/ min, the self-suspension ability of the ERC proppant has reached about 16 times that of the uncoated proppant. The performance of the above test between ERC proppant and other coated proppants was compared as shown in Table 1.

In order to test the thermal stability of self-suspension ability of the ERC proppant, we determined the self-suspension ability of the ERC and uncoated proppants at different temperatures. The same quality (0.5 g) of ERC proppant and uncoated ceramic proppant were poured into the guar gum solution (0.2 wt%) at different temperatures, and the stirring rate was controlled at 600 r/min. The proppant suspended on the surface of the solution was weighed and the its mass fraction was calculated, as shown in Fig. 9. As the temperature increases from 60 °C to 90 °C, the mass fraction of the ERC proppant suspended on the solution surface decreases from 74.26% to 60.24%, while the mass fraction of the uncoated proppant is only 7.32%—3.56%. Although the self-suspension ability of the ERC proppant decreases with an increase in temperature, more than 60% of the ERC proppant remain suspended on the surface of the solution when the temperature reaches 90 °C, indicating that the ERC proppant has excellent thermal stability of self-suspension ability.

4. Conclusions

A novel epoxy resin-coated (ERC) proppant with excellent self-

 Table 1

 Performance comparison of different coated proppants.

Туре	Surface roughness	Liquid conductivity	Surface adhesion force	Self-suspension ability
Phenolic resin-coated proppant (Xu et al., 2020) Directional adsorption coated proppant (Lan et al., 2020) Epoxy resin coated (ERC) proppant	smooth	60% higher than the uncoated ceramic proppant at 13.6 MPa pressure 30% higher than the uncoated ceramic proppant at 6.9 MPa pressure 16.71% higher than the uncoated ceramic proppant at 40 MPa pressure	ceramic proppant Higher than uncoated proppant	High self-suspension ability High self-suspension ability Super high self- suspension ability

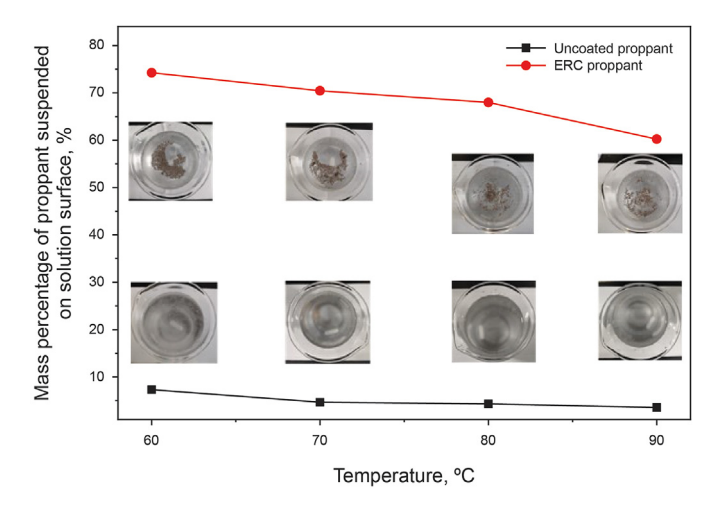


Fig. 9. Thermal stability of ERC and uncoated proppants.

suspension performance is prepared. Under the constant stirring rate, the self-suspension ability of this ERC proppant is nearly 16 times that of the uncoated proppants. Compared with the uncoated proppant, the ERC proppant maintains high lipophilicity while increases its hydrophobic properties by 83.8%. Besides, the adhesion force of the ERC proppant is also enhanced, making it easier adhere to the fracture surface, which can drastically improve the performance of proppant supporting the fractures, and improve the overall hydrocarbon recovery. Moreover, the liquid conductivity of the ERC proppant is 16.71% higher than the uncoated proppant at the closure pressures of 40 MPa. The proppant designed in this study is expected to be applied to shale fractures and promote the further development of proppant technology.

Acknowledgments

This research was supported by the National Key Research and Development Program (SQ2020YFC190006-02), National Nature Science Foundation of China (No. 51875577), Science Foundation of China University of Petroleum, Beijing (Nos. 2462019QNXZ02, 2462020YXZZ018).

Appendix A. Supplementary data

Supplementary data to this article can be found online at https://doi.org/10.1016/j.petsci.2021.09.004.

References

- Al-Muntasheri, G.A., Liang, F., Hull, K.L., 2017. Nanoparticle-enhanced hydraulic-fracturing fluids: a review. SPE Prod. Oper. 32 (2), 186–195. https://doi.org/10.2118/185161-PA.
- Barati, R., Liang, J., 2014. A review of fracturing fluid systems used for hydraulic fracturing of oil and gas wells. J. Appl. Polym. Sci. 131 (16), 318–323. https:// doi.org/10.1002/app.40735.
- Bogacki, J., Zawadzki, J., 2019. Multipurpose usage of magnetic proppantsduring shale gas exploitation. Ecol Chem Eng S 26 (1), 37–44. https://doi.org/10.1515/
- Cao, W., Xie, K., Lu, X., Chen, Q., Tian, Z., Lin, W., 2020. Self-suspending proppant manufacturing method and its property evaluation. J. Petrol. Sci. Eng. 192. https://doi.org/10.1016/j.petrol.2020.107251, 107251.
- Cao, W., Xie, K., Lu, X., Liu, Y., Zhang, Y., 2019. Effect of profile-control oil-displacement agent on increasing oil recovery and its mechanism. Fuel 237 (1), 1151–1160. https://doi.org/10.1016/j.fuel.2018.10.089.
- Chen, T., Wang, G.Z., Gao, J., Yang, Y.D., Ma, R., Lei, X.R., et al., 2012. Study on resin coated sand proppant used for oil production. Trans Tech Publ 524, 1910–1914. https://doi.org/10.4028/www.scientific.net/AMR.524-527.1910.
- Chen, Y., Nagaya, Y., Ishida, T., 2015. Observations of fractures induced by hydraulic fracturing in anisotropic granite. Rock Mech. Rock Eng. 48 (4), 1455–1461.

https://doi.org/10.1007/S00603-015-0727-9.

- Dong, K.J.C., He, W.H., Wang, M., 2019. Effect of surface wettability of ceramic proppant on oil flow performance in hydraulic fractures. Energy Sci Eng 7 (2), 504–514. https://doi.org/10.1002/ese3.297.
- Dong, X., Zhao, H., Li, J., Tian, Y., Zeng, H., Ramos, M.A., et al., 2020. Progress in bioinspired dry and wet gradient materials from design principles to engineering applications. iScience 23 (11), 101749. https://doi.org/10.1016/ iisci.2020.101749.
- Fan, J., Bailey, T.P., Sun, Z., Zhao, P., Uher, C., Yuan, F., et al., 2018. Preparation and properties of ultra-low density proppants for use in hydraulic fracturing. J. Petrol. Sci. Eng. 163, 100–1099. https://doi.org/10.1016/j.petrol.2017.10.024.
- Fu, L., Zhang, G., Ge, J., Liao, K., Li, T., Yu, M., 2016a. Study on a new water-inhibiting and oil-increasing proppant for bottom-water-drive reservoirs. J. Petrol. Sci. Eng. 145, 290–297. https://doi.org/10.1016/j.petrol.2016.05.025.
- Fu, L., Zhang, G., Ge, J., Liao, K., Pei, H., Li, J., 2016b. Experimental study of self-aggregating proppants: new approaches to proppant flowback control. Open Petrol. Eng. J. 9 (1), 236–246. https://doi.org/10.1016/j.petrol.2016.05.025.
- Gomez, V., Alexander, S., Barron, A.R., 2017. Proppant immobilization facilitated by carbon nanotube mediated microwave treatment of polymer-proppant structures. Colloid. Surface. 513 (5), 297–305. https://doi.org/10.1016/icolsurfa.2016.10.058
- Gu, M., Dao, E., Mohanty, K.K., 2015. Investigation of ultra-light weight proppant application in shale fracturing. Fuel 150 (15), 191–201. https://doi.org/10.1016/ifuel 2015 02 019
- Hu, W., Bao, J., Hu, B., 2013. Trend and progress in global oil and gas exploration. Petrol. Explor. Dev. 40 (4), 439–443. https://doi.org/10.1016/s1876-3804(13) 60055-5.
- Jia, C., Zheng, M., Zhang, Y., 2012. Unconventional hydrocarbon resources in China and the prospect of exploration and development. Petrol. Explor. Dev. 39 (2), 139–146. https://doi.org/10.1016/s1876-3804(12)60026-3.
- Jung, M.-H., Choi, H.-S., 2009. Characterization of octadecyltrichlorosilane self-assembled monolayers on silicon (100) surface. Kor. J. Chem. Eng. 26 (6), 1778–1784. https://doi.org/10.1007/s11814-009-0249-9.
- Kondash, A., Vengosh, A., 2015. Water footprint of hydraulic fracturing. Environ. Sci. Technol. Lett. 2 (10), 276–280. https://doi.org/10.1021/acs.estlett.5b00211.
- Kulkarni, M.C., Ochoa, O.O., 2012. Light weight composite proppants: computational and experimental study. Mech. Adv. Mater. Struct. 19 (1–3), 109–118. https:// doi.org/10.1080/15376494.2011.572241.
- Lan, W., Niu, Y., Sheng, M., Lu, Z., Yuan, Y., Zhang, Y., et al., 2020. Biomimicry surface-coated proppant with self-suspending and targeted adsorption ability. ACS Omega 5 (40), 25824–25831. https://doi.org/10.1021/acsomega.0c03138.
- Liang, F., Sayed, M., Al-Muntasheri, G.A., Chang, F.F., Li, L., 2016. A comprehensive review on proppant technologies. Petroleum 2 (1), 26–39. https://doi.org/ 10.1016/j.petlm.2015.11.001.
- Liu, H., 2011. Performance evaluation of selective proppant and its application in low-permeability fractured reservoir. Reserv Eval Dev Z 1 (1–2), 55–60. https://doi.org/10.13809/j.cnki.cn32-1825/te.2011.z1.010 (in Chinese).
- Liu, J., Cao, S., Wu, X., Yao, J., 2019. Detecting the propped fracture by injection of magnetic proppant during fracturing. Geophysics 84 (3), JM1–JM14. https:// doi.org/10.1190/geo2018-0221.1.
- Liu, P., Guo, S., Lian, M., Li, X., Zhang, Z., 2015. Improving water-injection performance of quartz sand proppant by surface modification with surface-modified nanosilica. Colloid. Surface. 470, 114–119. https://doi.org/10.1016/j.colsurfa.2015.01.073.
- Ma, X., Tian, Y., Zhou, Y., Wang, K., Chai, Y., Li, Z., 2016. Sintering temperature dependence of low-cost, low-density ceramic proppant with high breakage resistance. Mater. Lett. 180 (1), 127–129. https://doi.org/10.1016/j.matler.2016.04.09. OCT.
- Moghadasi, R., Rostami, A., Tatar, A., Hemmati-Sarapardeh, A., 2019. An experimental study of Nanosilica application in reducing calcium sulfate scale at high temperatures during high and low salinity water injection. J. Petrol. Sci. Eng. 179, 7–18. https://doi.org/10.1016/j.petrol.2019.04.021.
- Palisch, T., Duenckel, R., Wilson, B., 2015. New technology yields ultrahigh-strength proppant. SPE Prod. Oper. 30 (1), 76–81. https://doi.org/10.2118/168631-PA.
- Pangilinan, K.D., Al Christopher, C., Advincula, R.C., 2016. Polymers for proppants used in hydraulic fracturing. J. Petrol. Sci. Eng. 145, 154–160. https://doi.org/10.1016/j.petrol.2016.03.022, 2016.
- Samaha, M.A., Tafreshi, H.V., Gad-el-Hak, M., 2012. Superhydrophobic surfaces: from the lotus leaf to the submarine. CR Mecanique 340 (1), 18–34. https://doi.org/10.1016/j.crme.2011.11.002.
- Shiozawa, S., McClure, M., 2016. Simulation of proppant transport with gravitational settling and fracture closure in a three-dimensional hydraulic fracturing simulator. J. Petrol. Sci. Eng. 138, 298–314. https://doi.org/10.1016/ i.petrol.2016.01.002.
- Syakur, A., Hermawan, Sutanto, H., 2017. Determination of hydrophobic contact angle of epoxy resin compound silicon rubber and silica. IOP Conf. Ser. Mater. Sci. Eng. 190, 012025. https://doi.org/10.1088/1757-899x/190/1/012025.
- Tomac, I., Gutierrez, M., 2015. Micromechanics of proppant agglomeration during settling in hydraulic fractures. J Petrol Explor Prod Technol 5 (4), 417–434. https://doi.org/10.1007/s13202-014-0151-9.
- Wen, Q., Zhang, S., Wang, L., Liu, Y., Li, X., 2007. The effect of proppant embedment upon the long-term conductivity of fractures. J. Petrol. Sci. Eng. 55 (3–4), 221–227. https://doi.org/10.1016/j.petrol.2006.08.010.
- Witte, P.G., Bush, M.A., Scott, H.W., 2010. Propagation of a partial incomplete ossification of the humeral condyle in an American cocker spaniel. J. Small Anim.

- Pract. 51 (11), 591-593. https://doi.org/10.1111/j.1748-5827.2010.00988.x.
- Xu, Q., Fan, F., Lu, Z., Sheng, M., Tian, S., Zhang, Y., et al., 2020. Reversible adhesion surface coating proppant. Chin. Chem. Lett. 32 (1), 553–556. https://doi.org/10.1016/j.cclet.2020.02.014.
- Yan, J., Wang, F., 1993. Wettability alteration of silica induced by surfactant adsorption. Oilfield Chem. 10 (3), 195–200. https://doi.org/10.19346/ j.cnki.1000-4092.1993.03.001.
- Yang, J., Liu, X.-H., Meng, Q.-N. (Eds.), 2019. Development and Application of Double-Layer Coated Hydrophobic Proppant. Springer, pp. 2487–2495. https://
- doi.org/10.1007/978-981-15-2485-1_227.
- Zhang, J., Liu, K., Cao, M., 2017. Experimental study on modified polyacrylamide coated self-suspending proppant. Fuel 199, 185—190. https://doi.org/10.1016/j.fuel.2017.02.103.
- Zoveidavianpoor, M., Gharibi, A., 2015. Application of polymers for coating of proppant in hydraulic fracturing of subterraneous formations: a comprehensive review. J. Nat. Gas Sci. Eng. 24, 197–209. https://doi.org/10.1016/j.jngse.2015.03.024.